

1 *Review*

2 **DNA Aptamers for Functionalisation of DNA** 3 **Origami Nanostructures**

4 **Yusuke Sakai¹, Md. Sirajul Islam¹, Martyna Adamiak¹, Simon Chi-Chin Shiu²,**
5 **Julian Alexander Tanner² and Jonathan Gardiner Heddle^{1,*}**

6 ¹ Malopolska Centre of Biotechnology, Jagiellonian University; yusuke.sakai@uj.edu.pl (Y.S.);
7 md.sirajul.islam@uj.edu.pl (M.S.I.); martyna.adamiak@uj.edu.pl (M.A.); jonathan.heddle@uj.edu.pl (J.G.H.)

8 ² School of Biomedical Sciences, Li Ka Shing Faculty of Medicine, The University of Hong Kong;
9 simon.chichin.shiu@gmail.com (S.C.C.S.); jatanner@hku.hk (J.A.T.)

10 * Correspondence: jonathan.heddle@uj.edu.pl; Tel.: +48-12-664-6119

11

12 **Abstract:** DNA origami has emerged in recent years as a powerful technique for designing and
13 building 2D and 3D nanostructures. While the breadth of structures that have been produced is
14 impressive, one of the remaining challenges, especially for DNA origami structures intended to
15 carry out useful biomedical tasks in vivo, is to endow them with the ability to detect and respond
16 to molecules of interest. Target molecules may be disease indicators or cell surface receptors, and
17 the responses may include conformational changes leading to release of therapeutically relevant
18 cargo. Nucleic acid aptamers are ideally suited to this task and are beginning to be used in DNA
19 origami designs. In this review we consider examples of uses of DNA aptamers in DNA origami
20 structures and summarise what is currently understood regarding aptamer-origami integration. We
21 review three major roles for aptamers in such applications: protein immobilisation, triggering of
22 structural transformation, and cell targeting. Finally, we consider future perspectives for DNA
23 aptamer integration with DNA origami.

24 **Keywords:** DNA origami; aptamer; DNA nanotechnology; protein nano array; biosensor; logic gate;
25 enzyme cascade; drug delivery system; targeted therapy; molecular robotics

26

27 **1. Introduction**

28 Nucleic acid aptamers are typically 15-90 nucleotide lengths of single-stranded DNA, RNA or
29 modified nucleic acid, which can function similarly to antibodies – having the ability to bind to
30 molecular targets with high specificity and affinity. They are selected from a random sequence pool
31 according to affinity for a particular target by several rounds of selection and amplification in a
32 process known as Systematic Evolution of Ligands by EXponential enrichment (SELEX) (Figure 1)[1,
33 2]. This was originally carried out using RNA but single-stranded DNA (ssDNA) was shown to be
34 viable in work that developed a thrombin aptamer[3]. The use of DNA has a number of advantages
35 over RNA, notably higher chemical stability and obviation of a reverse transcription step during each
36 round of SELEX, concomitantly DNA aptamer development has grown rapidly[4]. Perhaps
37 surprisingly, although RNA has the additional 2'-hydroxyl group which imparts more diverse
38 secondary structures than DNA, successful aptamers of both types have been shown to have affinities
39 comparable to monoclonal antibodies (K_D in the range 0.1-50 nM[4]). Taking advantage of the fact
40 that aptamers are synthesised chemically, varieties of chemical modifications have been introduced
41 to the base, ribose and phosphate backbone to confer chemical stabilities, options for further chemical
42 conjugation and higher affinities[5]. For example, 2'-fluoro,2'-amino and 2'-O-alkyl substitution of
43 ribose are well-known to increase nuclease stability[6, 7] while introducing amino acid mimicking
44 bases has been demonstrated to expand chemical diversity of aptamer structures[8, 9].

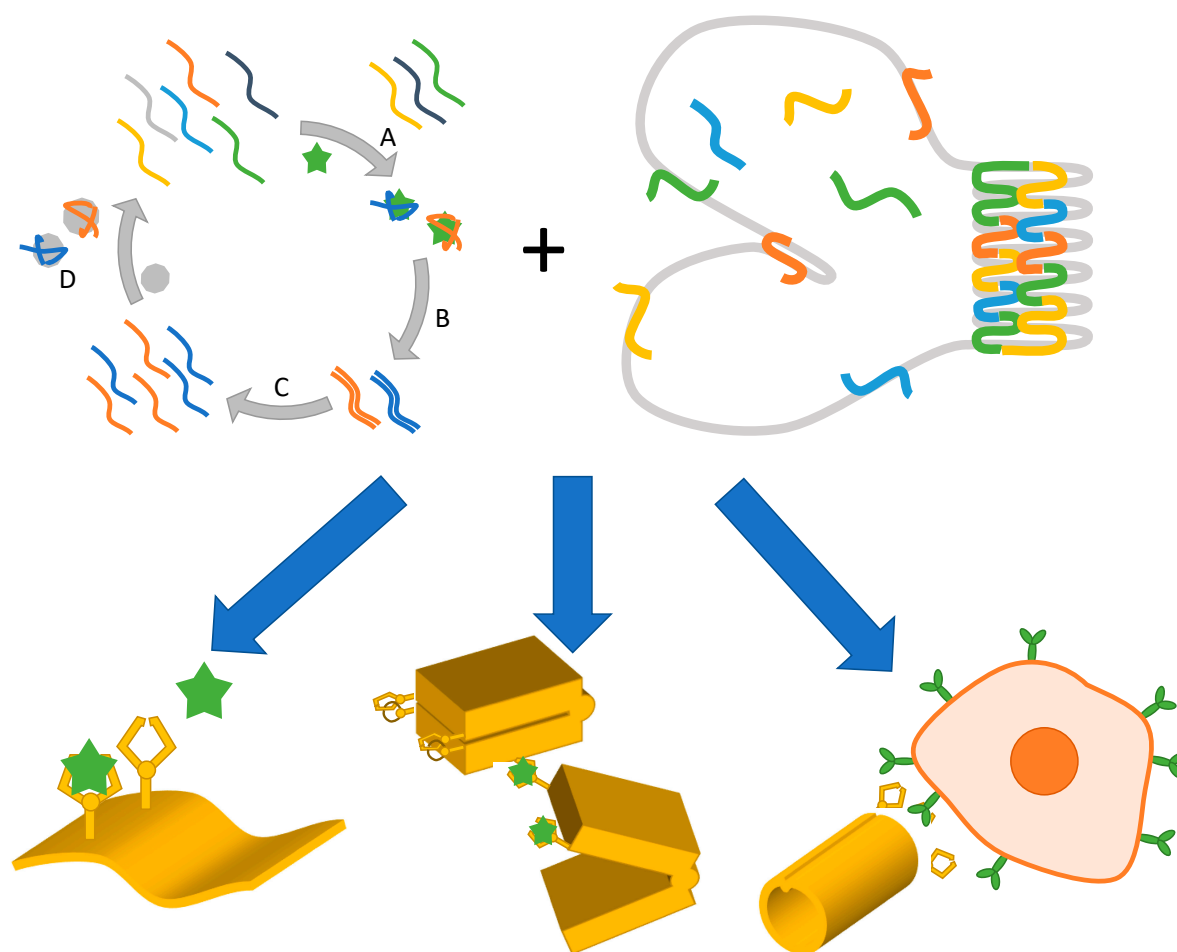


Figure 1. Applications of DNA aptamers when combined with DNA origami. (Top left) Schematic of the SELEX process. First, the fraction with target (green star) affinity is extracted from an initial ssDNA/RNA pool (A) and amplified by (reverse transcription and) PCR amplification (B). The reverse sequences are removed, or forward sequences are transcribed to prepare an enriched ssDNA or RNA library respectively (C) and occasionally counter selection is inserted to remove non-specific binding fractions according to affinity for counter target (grey circle) (D). The selected fraction is used as the second-generation library for the next round of selection (A). (Top right) Schematic illustration of DNA origami assembly. A long ssDNA (grey) is folded by hundreds of short ssDNA (coloured) by designed hybridization. Combination of aptamer and DNA origami (yellow) can result in: (Bottom left) protein nanoarray and biosensor construction via capture of target protein (green) by aptamer arm; (Bottom centre) Target dependent mechanical transformation by aptamer-lock or split aptamer integration for either biosensing or molecular computing; and (Bottom right) specific cell targeting for drug delivery and targeted therapy e.g. by utilising cancer cell targeting aptamers.

45 As for antibodies, aptamers have potential for targeted therapy, triggering cell signalling, or
 46 inhibition of the enzymatic activity of target molecules. Aptamers can be readily chemically
 47 synthesized and modified, leading to the expectation of reduced quality control costs for medical
 48 usage when compared to antibodies. Further advantageous characteristics of nucleic acid aptamers
 49 include flexibility of chemical modification, long storage period and low immunogenicity.
 50 Conjugation to other chemical entities has been demonstrated including chemotherapeutic agents,
 51 siRNA, nanoparticles, and solid phase surfaces for therapeutic and diagnostic applications[5]. A
 52 notable example of practical use is Macugen, an RNA aptamer that was the first Food and Drug
 53 Administration (FDA) approved drug used in the treatment of macular degeneration disease[10, 11].
 54 Several aptamer therapeutics for oncology have shown promise in pre-clinical models as well as

55 clinical trials[12]. Aptamers are also being developed that can be used as clot busters, cancer
56 therapies, autoantibodies, diabetes treatments, etc[13].

57 DNA origami (also herein referred to as simply “origami”) is a method whereby arbitrary 2D
58 and 3D nanoscale objects made from DNA can be designed and produced in a relatively
59 straightforward way (Figure 1) and was first introduced in 2006[14]. DNA origami structures are
60 made from a template strand of ssDNA, typically M13 phage genomic DNA which is folded into
61 shape by many (typically around 200) short staple strands which are complementary to linearly distal
62 sequences of the template strand. Maximisation of base-pairing to the staple brings the distal
63 sequences into close proximity and in this way a bespoke shape can be formed. DNA origami has
64 progressed rapidly and a breath-taking array of structures have been produced[15]. 2D DNA
65 origamis have been widely used, for example to produce nanoscale imagery[14, 16] as well as
66 structures with potential applications such as molecular pegboards[17-20] and molecular rulers [21,
67 22] and to produce heterogenous arrays of proteins in nanoscale wells[23]. 3D DNA origamis[24]
68 have been produced with a wide range of sizes, shapes and decorations. These have been shown to
69 be able to act as nanocontainers[25], immunomodulating agents[26], computational devices,
70 standards in electron microscopy[27], amongst many others.

71 As DNA origami and DNA/RNA aptamers are constructed from nucleic acid material they offer
72 an immediate compatibility with DNA origami whereby aptamers could be attached to any extended
73 staple sequence via base pairing or via simple extension of the staple sequence. Aptamers can
74 potentially be placed anywhere on a DNA origami structure with high resolution due to the fact that
75 the DNA helices in DNA origami structures are bundled tightly together with the centres of
76 neighbouring helices being only ca 2 nm apart and the phase of the double helical phosphate
77 backbone of the staple stands to which the aptamers attach repeats with a ca 3 nm pitch. It is also the
78 case that each staple strand could in theory be appended with a different bound molecule, allowing
79 for multiplexing of functionalities.

80 DNA aptamers have found a myriad of uses outside of DNA nanotechnology[28]. For example,
81 they have been attached to gold nanoparticles whereby the presence/absence of ligands such as lead,
82 adenosine, cocaine or mixtures can control the accessibility of complementary sequences on the
83 nanoparticles leading to “switching on” or “off,” resulting in observable colour changes[29, 30].
84 Aptamers responsive to ATP have been used to decorate polymers to deliver doxorubicin, an anti-
85 cancer drug, designed to be released in the cell due to ATP aptamer transformation[31, 32].

86 DNA origami research is a part of a vast field of DNA nanotechnology and there are numerous
87 reports of aptamer functionalised DNA nanostructures[33-38]. Though still at a relatively early stage,
88 three principles of successful aptamer integration design for DNA nanostructures have recently been
89 outlined: Shape – overall design of DNA nanostructure to define how and for what purpose aptamer
90 modules are integrated; Self-Complementarity – an indispensable optimisation step to control
91 equilibration between the two states of the aptamer in presence or absence of target molecule; Spatial
92 Flexibility – optimal positioning of aptamers to give accessibility and/or space for the DNA
93 nanostructure itself to undergo dynamic movement[39]. As more aptamers are developed, they will
94 represent a growing library of motifs that may be incorporated into DNA origami structures. Here,
95 we highlight specific examples of DNA origami research as well as milestone reports of individual
96 methodologies to give a snapshot of current research and future perspectives of the marriage between
97 DNA origami and nucleic acid aptamers.

98 Overall, DNA and RNA aptamers offer significant opportunity for facile attachment to designed
99 DNA origami structures in order to endow them with useful functionality. Existing research points
100 at the possible categories of aptamer modifications that may be used and these include i) aptamers to
101 immobilise target molecules, as demonstrated by nanoarrays as well as biosensor applications
102 (Figure 2); ii) using aptamers to trigger DNA nanostructure conformational changes aimed at either
103 biosensor or molecular computing outcomes (Figure 3); iv) using aptamers for (cancer) cell targeting
104 for drug delivery (Figure 4).

105

106 2. Aptamers for Target Immobilization

107 DNA nanotechnology offers an exquisite method for producing bottom-up nanoarrays, i.e. it
108 can be used to organize various particles in spatially defined patterns with nano-meter precision via
109 self-assembly, as first demonstrated by the construction of simple nanostructures of gold
110 nanoparticles precisely arrayed on a DNA helix[40]. Using biotinylated DNA has allowed templated
111 nanoarrays to expand to include streptavidin[41] and streptavidin coupled antibodies [42]. A more
112 universal methodology of DNA based protein nanoarray formation was subsequently shown[43]
113 where a 15 nt thrombin aptamer (HD1)[3] was successfully introduced which precisely arrayed
114 thrombin on triple-crossover DNA tiles as observed by atomic force microscopy (AFM). These
115 arrayed nanoparticles are typically visualised by AFM as dot(s) of appropriate height on regularly
116 patterned DNA nanostructures as if pegged by aptamers on pegboard made of DNA.

117 In 2007, just after the introduction of the DNA origami method, the platform of aptamer based
118 protein nano-arrays was expanded from DNA tiles[43] to DNA origami (Figure 2A)[17]. A platelet
119 derived growth factor (PDGF) aptamer (36t)[44] and a thrombin aptamer (HD22)[45] were each
120 arrayed on a rectangular DNA origami structure with nanometre precision. This multivalent aptamer
121 system was further systematically investigated[46]: one target molecule was captured on the DNA
122 nanostructure by two aptamers recognising different epitopes using another thrombin aptamer
123 (HD1)[3]. Utilising the precise addressability inherent to DNA nanostructures, 4-helix bundle or 5-
124 helix bundle DNA tiles and rectangular DNA origami, were arrayed with two thrombin aptamers
125 with a separation varying from 2 to 6.9 nm in order to seek the optimal interval for the efficient
126 binding of thrombin, verified by EMSA. A four-thymine spacer was added to the ends of the
127 aptamers to increase flexibility. As the two aptamers recognise opposite sides of the ca 4.1 diameter
128 protein simultaneously, the optimal spacing of the aptamers was found to be 5.3 nm, i.e. four dsDNA
129 helices. Combining a microfluidics system and the DNA origami with dual thrombin aptamers
130 resulted in a biosensor system for rapid detection of thrombin from cell lysate (Figure 2B)[47]. In this
131 work, a simple crossed microchip for isotachopheresis was prepared, where a mixture of DNA
132 origami and thrombin spiked cell lysate was electrophoresed and concentrated between the loading
133 electrolyte (LE) and the trailing electrolyte (TE). The concentrated fraction of DNA origami-thrombin
134 complex was then extracted from the cross section of the microfluidics chip and confirmed by AFM.
135 Successful thrombin detection from cell lysate spiked with 15 nM thrombin was achieved. Recently,
136 all atom molecular dynamics studies were performed to simulate the binding behaviour of a dual
137 thrombin aptamer system with a 1152 nt scaffold small DNA origami structure, 26 nt thrombin
138 aptamer (NU172, also known as ARC2172)[48] and 29 nt-long thrombin aptamer (HD22)[49].
139

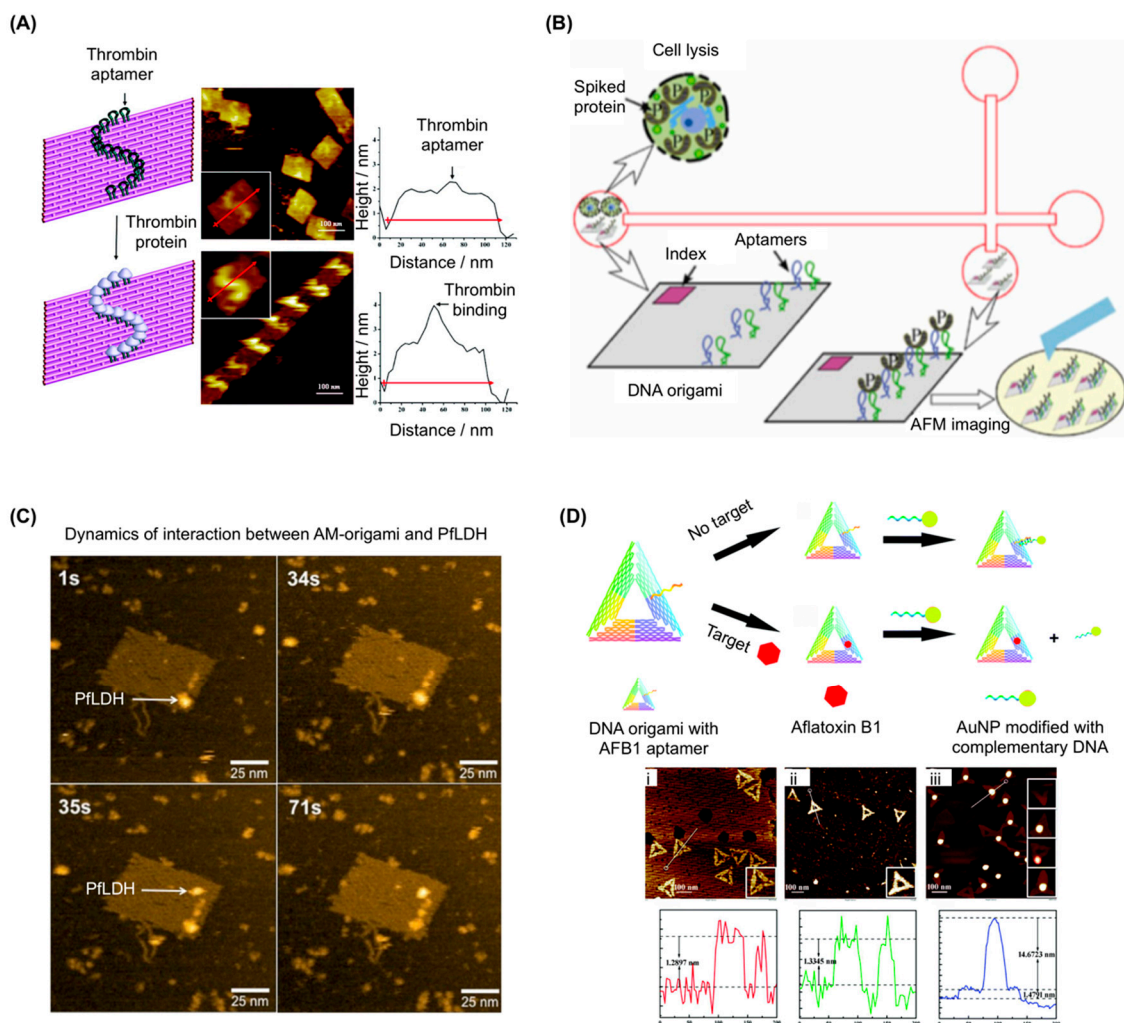


Figure 2. Examples of aptamer use in target immobilization on DNA origami. (A) (left) Schematic showing an S-shaped pattern of thrombin templated on DNA origami. Grey balls represent thrombin proteins. (middle) Images corresponding to the arrays shown on the left, with zoomed-in images (inset); (right) line cross-section analysis of the AFM images show an increase in the height at the sites of protein binding. Adapted with permission from Chhabra et al [20]. Copyright (2007) American Chemical Society. (B) Schematic for stacking, separation and identification of DNA origami and its protein binding using ITP in a cross-channel microfluidic chip fabricated in fused silica. DNA origami with bivalent aptamers was assembled by replacing individual staple strands. Thrombin was used as the target analyte to provide functional validation. After incubating origami in thrombin-spiked cell lysate, separation was performed by on-chip ITP and verified by direct visualization with atomic force microscopy (AFM). Adapted with permission from Mei et al, *Nano Res.*, 2013 [47]. (C) HS-AFM images showing dynamics of interaction between AM-origami and PflDH. At 1 s, a single AM-origami is visible with one PflDH (indicated by white arrow) attached to the aptamer-modified region. At 35 s a second PflDH (indicated by white arrow) binds to the region and both proteins remain in place beyond 71 s. Adapted from Godonoga et al. [50]. (D) (top) Schematic illustration of the analytical principle of the aptamer-tagged DNA origami/complementary ssDNA–AuNPs system for detecting AFB1; (bottom) AFM images with section plots of aptamer-tagged triangular DNA origami nanostructures before and after binding. (i) Aptamer-tagged triangular DNA origami; (ii) aptamer-tagged triangular DNA origami after binding with AFB1; (iii) aptamer-tagged triangular DNA origami after hybridization with the

AuNP-conjugated ssDNA. From Lu et al, Chem. Commun., 2017 [51] – Reproduced by permission of The Royal Society of Chemistry.

140 Rothmund's rectangular DNA origami structure has been utilised by several groups as a basis
141 for pegboard biosensor construction. For example, dual thrombin aptamers (HD1 and HD22),
142 inactivated by an O⁶-methyl modification of guanine base in advance, have been used to detect the
143 activity of the DNA repair enzyme, human O⁶-alkylguanine-DNA alkyltransferase (hAGT)[52].
144 When the sample mixed with the biosensor has demethylation activity, the original sequence of the
145 thrombin aptamer is recovered and it will immobilise thrombin on DNA origami, which is visible in
146 AFM. As inhibition of hAGT can enhance the cytotoxicity of alkylating agents in tumour cells, this
147 system has potential use in screening inhibitors as candidate chemotherapy enhancers. In another
148 example[50] we developed a DNA origami biosensor with potential for malaria detection by
149 integrating recently discovered *Plasmodium falciparum* lactate dehydrogenase (PfLDH) aptamers
150 (2008s) (Figure 2C)[53] which are notable as PfLDH is a biomarker of malaria infection. Twelve
151 PfLDH aptamers were arrayed on a DNA rectangle via 20 nt poly T linkers and specific binding of
152 PfLDH was observed using AFM and high-speed AFM (HS-AFM) measurements. Although the
153 affinity was decreased when the aptamer was connected to staple strands (Native $K_D \sim 56 \pm 18$ nM,
154 staple connected: $K_D \sim 600$ -1100 nM), the aptamer modified DNA rectangle selectively captured
155 PfLDH at concentrations as low as 500 nM and functioned even in presence of blood plasma.
156 Captured PfLDH retained enzymatic activity allowing biochemical detection using methods other
157 than AFM imaging. Others have constructed a DNAzyme-operated logic gate system able to release
158 a detectable analyte only in the presence of certain DNA strands[54]. In these conditions, a DNA
159 sequence on the DNA origami surface was cleaved by a DNAzyme, leading to ssDNA release. The
160 released DNA could be pre-labelled with detectable moieties such as ruthenium dye and gold
161 nanoparticles (AuNP). Protein capture and programmed release was demonstrated by incorporating
162 the thrombin aptamer (HD1) into the cleavable strand[54] with released thrombin being detectable
163 e.g. via SDS PAGE.

164 A NOT gate was constructed on a triangular DNA origami structure to detect the small
165 molecule, aflatoxin B1 (AFB1), using the pegboard based detection method (Figure 2D)[51]. Here
166 staple strands were modified with a AFB1-binding aptamer[55] sequence. In the absence of AFB1, a
167 complementary sequence with a AuNP attached was able to hybridise to the aptamer, detectable via
168 AFM and gel electrophoresis. If AFB1 is present, it is bound by the aptamer meaning that the gold-
169 labelled strand cannot bind. This NOT gate system enables detection of a small molecule target that
170 is not visible in AFM. Other alternatives to microscope imaging-based methods for detecting binding
171 to aptamers on origami have been demonstrated with one example using surface plasmon resonance
172 to evaluate the interaction of a 3D DNA origami structure with thrombin aptamer (HD22) and
173 thrombin[56].

174 Since aptamers can precisely localise proteins onto the surface of DNA origami, we foresee that
175 this will be a useful approach for biophysical characterisation of enzymes and for nanoreactors.
176 Similar ideas have been demonstrated using protein-DNA conjugates on various designs of origami.
177 For example, glucose peroxidase and horseradish peroxidase have been physically coupled through
178 origami for peroxidation of ABTS or TMB resulting in signal generation, as reviewed in 2017[57].
179 Since DNA origami is highly programmable, the functionalisation of this enzyme cascade could be
180 optimized through varying the spacing distance between enzymes, thereby providing insight into
181 mechanism[58].

182 As aptamers can be defined as single-stranded nucleic acids binding specifically to a target,
183 known sequences which bind to a specific protein could also be regarded as aptamers. The Morii
184 group has developed Zinc-finger[59] or leucine-zipper[60] based DNA binding motifs to array target
185 proteins on DNA nanostructures. In 2016, they created an artificial enzyme cascade by incorporating
186 binding sites for xylose reductase and xylitol dehydrogenase at specific locations on DNA origami
187 [61]. Both binding sites were single stranded DNA and one of them had a benzylguanine modification
188 on thymine for binding to xylitol dehydrogenase. This design of origami resembled the xylose
189 metabolic pathway. Enzymatic activity resulting in generation of xylulose and NADH could also be

190 controlled through modulating inter-enzyme distances. Recent work from the same group also
 191 demonstrated the use of zinc-finger protein adaptors consisting of single-stranded hairpin structures
 192 for the binding of Kir3 K⁺ channel proteins[62]. The precise fabrication allowed design of various
 193 cavities in the DNA origami such that K⁺ channel current activity could be controlled by the
 194 oligomerization state of the protein complex. With more aptamers being developed against different
 195 targets, such approaches point towards particular promise for aptamers integrating with DNA
 196 origami potentially having the ability to modulate membrane protein activity.

197 In summary, DNA origami has expanded the concept of protein nanoarrays which was formerly
 198 investigated only on relatively smaller DNA nanostructures. Combining AFM visualisation and
 199 simple logic gates, a series of biosensor devices have been proposed targeting thrombin, PDGF, hAGT
 200 activity, PflLDH and AFB1. Challenges include the fact that integration of aptamers into DNA
 201 nanostructures may suppress the affinity for target due for example, to the sequence extensions
 202 required for connection to the larger structure, imperfect DNA origami assembly and steric hindrance
 203 for target molecule which can be partially recovered by optimising aptamer positioning and linker
 204 length. Combining simple logic gates with aptamers enables detection of aptamers targeting small
 205 particles which may be too small to be easily detectable in AFM imaging. A summary of aptamers
 206 used in conjunction with DNA origami are given in Table 1.
 207

Table 1. Summary of aptamer utilised in DNA origami research

Name	Target	Sequences	Length / DNA or RNA	Employed by	Ref
HD1	Thrombin (exosite I)	GGTGGTGTGGTTGG	15nt ssDNA	[46, 47, 52, 54]	[3]
HD22	Thrombin (exosite II)	AGTCCGTGGTAGGGCAGGTTGGGGTGACT	29nt ssDNA	[17, 49, 52, 56]	[45]
NU172 ¹	Thrombin	CGCCTAGGTTGGGTAGGGTGGTGGCG	26nt ssDNA	[49]	[48]
36t	PDGF	CACAGGCTACGGCACGTAGAGCATCACCAT GATCCTGTGT	40nt ssDNA	[17]	[44]
41t	PDGF	TACTCAGGGCACTGCAAGCAATTGTGGTCCC AATGGGCTGAGTAT	45nt ssDNA	[63-65]	[44]
SL12	VEGF	ATACCAGTCTATTCAATTGGGCCCGTCCGTAT GGTGGGTGTGCT ³	44nt ssDNA	[65]	[66]
TE17	CCRF-CEM cell	CAGCTACGCAATACAAACTCCGAACACCT GCTTCTGACTGGGTGCTG	48nt ssDNA	[63]	[67]
sgc8c	PTK7	ATCTAACTGCTGCGCCCGGGAAAATACTG TACGGTTAGA	41nt ssDNA	[63]	[68, 69]
2008s	PflLDH	CTGGGCGGTAGAACCATAGTGACCCAGCCGT CTAC	35nt ssDNA	[50, 70]	[53]
AFB1 aptamer	AFB1	GTGGGGCACGTGTTGTCTCTCTGTGTCCTCGTG CCCTTCGCTAGGCCAC	49nt ssDNA	[51]	[55]
ATP aptamer	ATP	ACCTGGGGGAGTATTGCGGAGGAAGGT ⁴	27nt ssDNA	[71-73]	[74, 75]
ATP aptamer	ATP	1: CTAcUACCTGGGGGAGTAT ⁵ 2: TGCGGAGGAAGGTcUAG	43nt ssDNA	[76]	[77]
aptakiss and GTP switch	GTP	aptakiss: UGCUCGGCCCCGCGAGCA GTPswitch: UCCGAAGUGGUUGGGCUGGGGCGUGUGAA AACGGA GTPswitch mutant: UCCGAAGUGGUUGGGCUGGGGCGUGUGAAA ACGGA	18nt RNA/35nt RNA/34nt RNA	[78]	[79]
S2.2	MUC-1	GCAGTTGATCCTTTGGATACCCTGG	25nt ssDNA	[80, 81]	[82]

cocaine aptamer	cocaine	GGGAGACAAGGATAAAATCCTCAATGAAGT GGGTCTCCC ⁶	39nt ssDNA	[72, 73]	[83]
AS1411 ²	Nucleolin	GGTGGTGGTGGTTGTGGTGGTGGTGG	26nt ssDNA	[84]	[85, 86]
C2NP	CD30	ACTGGGCGAAACAAGTCTATTGACTATGAGC	32nt ssDNA	[87]	[88]
zif268 binding site	zif268	CTGCGTGGGCGTGTTTTACGCCCCACGCAG	30nt ssDNA	[57, 59, 62]	[59]
AZP4 binding site	AZP4	CTTACGTGGCATGTTTCATGCCTCGTAAG	29nt ssDNA	[59, 62]	[59]
GCN4 binding site	GCN4	CTTCATGAGTCATGCGTTTTTCGCATGACTCAT GAAG	36nt ssDNA	[57, 60]	[60]

¹ Also known as ARC2172.

² Also known as AGRO100.

³ Derivative of VEa5[89].

⁴ In [71, 73], single G at 3' end was added as a result of optimisation.

⁵ Split aptamer. *cU* in the sequences are *dye modified nucleosides*.

⁶ Derivative of MNS-4.1[90].

208 3. Aptamers for controlling DNA origami structural changes

209 Molecular recognition by aptamers is accompanied by conformational change. By optimising
 210 the equilibrium between the partially complementary strand hybridisation and target-aptamer
 211 binding, aptamers behave as a molecular switches, converting the detection of specific target
 212 molecules into structural changes of DNA, which can be further converted to detectable outputs such
 213 as fluorescence signal shifts (Figure 3A)[91]. If such aptamer modules are included in DNA
 214 nanostructures, aptamer-target interaction can be made such that it results in release of the strand
 215 complementary to the aptamer strand, leading to dynamic transformation of the overall structure
 216 (Figure 3B). Where aptamers already consist of two moieties[79] or have been split by design[92],
 217 they can be reconstituted into a single complex in presence of target molecule. When each moiety of
 218 such an aptamer module is integrated to a distal site on the DNA nanostructure, molecular
 219 recognition brings the two parts together. In this way, aptamers can be used to actuate motion in
 220 DNA origami systems in response to specific molecular signals and different aptamers in parallel can
 221 be used to instantiate logic gates. To date, a number of DNA origami structures have demonstrated
 222 the use of aptamers in this way as described below.

223

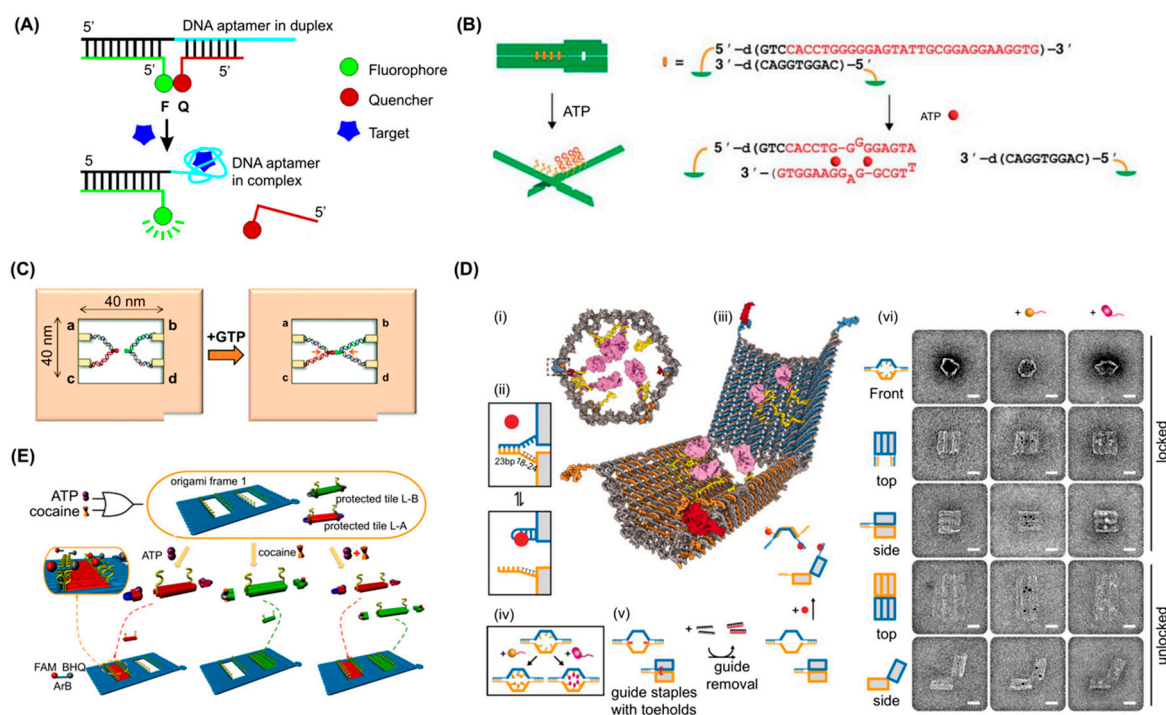


Figure 3. Examples of aptamer use in controlling DNA origami structural change. (A) Schematic for designing aptamer-based fluorescent reporters that function by switching structures from DNA/DNA duplex to DNA/target complex. Adapted with permission from Nutiu et al [91]. Copyright (2003) American Chemical Society. (B) Key and lock system to detect ATP using aptamer-based elements. Adapted from Kuzuya et al [71]. (C) Schematic of the system for investigating the interaction of kissing RNA aptamers using a DNA frame. Incorporation of the aptakiss into the a–c site and KG51 or GTPswitch into the b–d site in the DNA frame. When the GTPswitch is incorporated into the DNA frame, GTP should induce conformational change from the double-loop to the X-shape. From Takeuchi et al, [78] – Reproduced by permission of The Royal Society of Chemistry. (D) (i) Schematic of the front view of a closed nanorobot loaded with a protein payload; (ii) the DNA aptamer (blue) and a partially complementary strand (orange) make the aptamer lock. The lock can be stabilized in a dissociated state by its antigen key (red); (iii) mechanism of nanorobot opened by protein displacement of aptamer locks. The two domains (blue and orange) are constrained in the rear by scaffold hinges; (iv) Payloads (gold) and antibody Fab’ fragments (magenta) can be loaded inside the nanorobot; (v) Front and side views show guide staples (red) bearing 8-base toeholds that aid assembly of the nanorobot. After folding, guide staples are removed by addition of fully complementary oligos (black). Nanorobots can be subsequently activated by interaction with antigen keys (red); (vi) TEM images of robots in closed and open conformations. From Douglas et al [63]. Reprinted with permission from the American Association for the Advancement of Science. (E) Schematic illustration of the “OR” gate using ATP and cocaine as two independent inputs to trigger the filling patterns. In the locking step, both tile A or B can be deactivated by hybridizing with the protector strands PA or PB, which contain aptamer-recognizing sequences of ATP and cocaine in the middle region, respectively. In the unlocking step, the protector strands (PA or PB) at the ends of the L-A or L-B can be removed by adding the aptamer target (ATP or cocaine). Adapted with permission from Yang et al [72]. Copyright (2016) American Chemical Society.

224 3.1. Functionalised DNA origami with potential as biosensors

225 A biosensor oriented nanomechanical DNA origami structure was initially reported in 2011
 226 (Figure 3B)[71]. This design consisted of a pliers-shaped or scissors-shaped DNA origami
 227 nanostructure of two DNA origami bars covalently connected at their two centres by single

228 crossovers and one to four pairs of sensory modules including ATP aptamers[74, 75]. The aptamer
229 and its complementary strands formed four pairs of “aptamer locks” to convert the DNA nano-pliers
230 from an open X-shape to a closed parallel bar shape. In presence of 1 mM ATP, mimicking cellular
231 concentrations, the aptamer module captures ATP, releasing the complementary strand, resulting in
232 a decrease of the fraction of closed form DNA pliers from 72% to 40%. Target specificity was
233 confirmed using GTP as negative control. One to four pairs of telomere elements were also integrated,
234 these dimerize and form a G-quadruplex in the presence of sodium (or potassium) ions. The modules
235 acted as a zipper to close the DNA nanostructure from X form to parallel form in the presence of
236 sodium or potassium ions. Thus, the dynamic DNA origami structure converted binding of small
237 ligand to target aptamer mechanical transformation (opening or closing) of a large DNA origami
238 measurable by AFM imaging at a single molecular level or via a real-time fluorescence spectrum shift
239 of fluorescence resonance energy transfer (FRET) in bulk.

240 A mechanochemical DNA origami device utilising a PDGF aptamer was demonstrated in
241 2014[64]. In this approach, a 7-tile DNA origami nanostructure was designed in which the recognition
242 elements interlock adjacent tiles. The binding of a target to any of the recognition elements releases
243 the lock, which generates a change in the mechanical force signal, constantly measured by optical
244 tweezers. A PDGF aptamer[44] was used as the first recognition element in each of the six interlocks.
245 The detection sensitivity of the 7-tile origami device was as low as 10 pM within 10 min, improving
246 from 100 pM within 30 min[93] for a former single-interlock system, implying the arrangement of
247 multiple sensor units in series enhanced both the detection limit as well as detection time. A
248 multiplexing capacity of the platform by integrating a pair of DNA hybridisation locks with toehold
249 sequence and an aptamer lock together into the same device simultaneously was also
250 demonstrated[94]. DNA origami and aptamers have been combined to observe RNA kissing complex
251 formation with single molecule resolution[78]. To do this, a frame-shaped DNA origami structure
252 was designed with the two RNA sequences on opposite sides of a central hole. One sequence was a
253 designed aptamer motif (GTPswitch) which binds to the other moiety (aptakiss) responding to the
254 presence of GTP [79]. Before addition of GTP, both aptamers were visible in AFM as discrete
255 structures, forming a double loop shape. This became an X-shape after the addition of GTP (Figure
256 3C)[78]. The GTPswitch sequence was optimised to attain a statistically significant detection of 1 mM
257 GTP ($65.2 \pm 0.5\%$ from $44.0 \pm 2.0\%$ in absence of target molecule) and discrimination against ATP
258 ($46.4 \pm 2.5\%$ X-shape in presence of 1 mM ATP) meaning that GTP detection at a single molecule level
259 was achieved.

260 As DNA origami is a modular methodology, many groups have introduced various aptamers
261 into established structures for further functionalisation. For example, a split aptamer able to bind two
262 molecules of ATP[77] was introduced into the nanomechanical DNA origami pliers[76]. The
263 aptamers were labelled with different dyes such that a FRET fluorescence spectrum shift would occur
264 if the dyes approached each other (i.e. if the pliers closed). In the presence of 0.1 mM to 1 mM ATP,
265 the split aptamers bound ATP, reconstituting the native aptamer and closing the DNA pliers,
266 resulting in successful detection of ATP by FRET in real-time, confirmed by AFM and agarose gel
267 electrophoresis. Aptamers may have a use in targeting DNA origamis to cancer cells and a set of
268 aptamers for cancer-specific Mucin 1 protein (MUC-1) [82] have been integrated into a spherical DNA
269 origami structure[95]. In the system, two hemispheres are connected by single crossover and five
270 pairs of ssDNA evenly protrude from equatorial helices of both hemispheres. After assembling the
271 opened structure, each pair of the ssDNA overhangs are interlocked by lock strands containing a
272 centrally positioned MUC-1 aptamer sequence. In presence of the “key”, i.e. the target protein or the
273 complementary strand for the lock strands, the lock strands are removed from the DNA
274 nanostructure, leading to opening of the sphere. The device was demonstrated as opening on
275 exposure to MUC-1-containing cell lysate[81]. Other aptamers used in relation to disease treatment
276 or detection include the PflDH aptamer[53] which has been shown to work as part of a malaria
277 biosensor/prototype therapeutic delivery system whereby the aptamers control the opening of a DNA
278 origami box.[70] In this work two pairs of aptamer lock with partially complementary strands were
279 integrated between the lid and main box. The conformational change of the PflDH aptamer on

280 binding PflDH competes with the duplex formation closing the box lid. In absence of the target
281 molecule or presence of negative control (human LDH-B), the boxes with aptamer locks showed
282 mostly closed conformation (20% of DNA box open according to TEM imaging) while in presence of
283 100 nM PflDH, DNA box opened reaching ca 70% in the open form during 120 min of incubation.
284 Opening of the box by FRET based kinetics was also monitored. Due to the complementary strands
285 locking the lid, the estimated K_D of the aptamer was 655 nM, weaker than native aptamer with K_D of
286 approx. 42 nM.

287 3.2 DNA origami for Molecular Computing

288 Production of programmable DNA origami machines is a major goal. Indeed, many of the
289 aptamer -operated origami structures to date respond only if aptamer binds to signal and so could
290 be said to be a form of Boolean logic gate. However, beyond the largely sensory modules described
291 above, aptamer integration has offered more sophisticated programmability to DNA origami
292 structures[31, 32, 96].

293 One of the most innovative examples was demonstrated in 2012[63]. Here, a capsule-shaped
294 structure with two pairs of different aptamer locks closing the shape was designed (Figure 3D) and
295 a PDGF aptamer (41t)[44], protein kinase 7 aptamer (Sgc8c)[68, 69] and CCRF-CEM cell targeting
296 aptamer (TE17)[67] used. A cargo of up to 12 antibody (fragments) were encapsulated to target the
297 nanorobot to specific cells displaying antigen receptors, enabling the DNA origami structure to
298 discriminate cell types amongst Burkitt's lymphoma, acute myeloblastic leukemia, aggressive NK
299 leukemia, T-cell leukemia, acute lymphoblastic leukemia and neuroblastoma. Cells not expressing
300 the molecular "keys" to open the aptamer locks were not bound by the loaded DNA origamis, while
301 cells expressing the keys were, due to opening of the structure and exposure of the antibody
302 fragments. By using two different aptamer locks on a single DNA origami structure, an AND gate
303 could be constructed whereby the capsule would open only in the presence of both molecular keys.
304 Due to fluorescence labelling of the antibody fragments, the binding of DNA origami to target cell
305 types could be verified by FACS[63]. It is interesting to note that a high yield of closed DNA origami
306 structures was obtained by using additional "guide" staple strands to help set the closed state. These
307 could subsequently be removed prior to interaction with target. In this way a yield of 97.5% of closed
308 conformation was achieved.

309 The logic gate system, was subsequently expanded to include more sophisticated
310 programmability ex-vivo as well as in vivo using a cockroach model[65]. A barrel-shaped
311 encapsulating DNA origami structure similar to that described above was designed and PDGF
312 aptamer (41t) and vascular endothelial growth factor (VEGF) aptamer (SE12)[66] locks were used to
313 produce an effector robot (E) with an AND gate. Then a positive regulator (P) DNA origami was
314 constructed, which was loaded with ssDNA complementary to one of the locking strands of the
315 effector such that binding of the two robots opens E regardless of aptamer-ligand interaction.
316 Similarly, a negative regulator (N) was constructed which carries two ssDNAs complementary to two
317 locks on opposite sides of E, keeping it closed regardless of aptamer-ligand interaction. With a
318 different toehold sequence present on the locking strands, a secondary effector robot (F), which is
319 sensitive to PDGF and VEGF but is not activated or inactivated by positive or negative regulators,
320 was also introduced. Combining P, N and F robots in addition to the original nanorobot with an AND
321 gate behaviour resulted in successful emulation of AND, OR, XOR, NAND, NOT, CNOT and half
322 adder logic-gates.

323 Other logic-gate systems have been implemented in DNA origami to detect molecules of interest.
324 For example a DNA origami frame was produced containing two holes which could be filled by DNA
325 tiles in the presence of predefined target molecules, in this case ATP and cocaine (Figure 3E)[72]. The
326 DNA tile modules are inactivated by aptamer-locks[83, 90] which prevent them from filling the holes,
327 but in the presence of ATP or cocaine, the aptamer locks are released from the DNA tiles activating
328 sticky ends that have complementarity to sequences lining the holes. Whether the holes are unfilled
329 or filled can be detected by AFM. In this system the design elegantly included a mechanism whereby
330 detection could be achieved without requiring AFM. To do this a DNzyme (Mg^{2+} -dependent E6-

331 type DNAzyme-1) was reconstituted when the tiles bound into the holes. The reconstituted
332 DNAzyme cleaved a fluorescent reporter which included a fluorophore and quencher such that
333 active DNAzyme resulted in an increase in fluorescent signal. Combinations of these reporter systems
334 enabled emulation of OR, YES and AND logic gates using ATP and cocaine as input signals.

335 A second ATP/cocaine aptamer based logic gate nano-system[73] has been demonstrated which
336 utilises hexagonal DNA nanostructures[97] that can connect to each other laterally via aptamer locks.
337 four pairs of aptamer locks were embedded to connect two hexagonal DNA origami structures via
338 side-by-side dimerization and dissociation of the structure was optimised. As a result, the yield for
339 the dimeric form of the structure reached 89% which was decreased to 24% in presence of 5 mM ATP
340 in 2 hr. Similarly, the cocaine aptamer lock was used to mediate dimerization with dimer constituting
341 87% and 33% of the total in the absence or presence of 5 mM cocaine respectively. Finally, combining
342 the two aptamer locks formed a DNA origami trimer. Each DNA origami monomer was labelled by
343 0 to 2 streptavidin flags to distinguish them. The trimer was designed to dissociate into dimer and
344 monomer in presence of either ATP or cocaine or to dissociate into monomer in presence of both
345 signals. The DNA origami trimer was produced with 80% yield, which decreased to 19% in the
346 presence of either ATP or cocaine and to 2.8% in presence of both signals. The dimeric form (approx.
347 40%) observed in presence of either signal clearly demonstrated controlled dissociation with low
348 crosstalk

349 Overall, aptamer locks and split aptamers offer the capability for dynamic transformation of
350 DNA origami structures that can produce a response as a result of target molecule recognition. As a
351 biomarker device, the detection of target molecules such as ATP, Na⁺, K⁺, GTP, PDGF, cocaine and
352 PflDH have been converted to dynamic transformations of DNA origami structures, as evaluated by
353 AFM or TEM, optical tweezers, as well as agarose gel electrophoresis or tracked real-time by
354 fluorescence signal alteration, derived from FRET or quenchers. As each DNA nanostructure can
355 possess more than one aptamer module, AND gates can be easily constructed by integrating
356 orthogonal aptamer modules. Designing sequential reactions of DNA origami structure interactions,
357 allows various kinds of logic gate to be demonstrated. In all cases, high efficiency of transformation
358 control is challenging. Aptamer sequences themselves, along with complementary sequences and the
359 position and multivalency of aptamer modules need to be further optimised for improved
360 performance.

361 4. Aptamers for Cell Targeting

362 Analogously to their protein antibody counterparts, DNA aptamers have been developed which
363 bind to specific receptors that are displayed on the surface of certain cell types (e.g. cancer cells)[98].
364 In some cases, aptamers binding to these receptors can promote uptake of the conjugated structures
365 by the cell as well as triggering cellular signals. This has been utilised in a number of cases to target
366 DNA nanostructures to specific cells with therapeutic goals, as has recently reviewed by Kim et al.
367 including a useful table of cell selectivity of aptamers[99]. Sgc8c, also used in the programmable DNA
368 origami robot mentioned above,[63] targets protein tyrosine kinase 7 (PTK7), a transmembrane
369 receptor highly expressed in cancer cell lines including T-cell acute lymphoblastic leukemia[69]. The
370 MUC-1 aptamer, S2.2, also used in the DNA nanosphere work[81], targets MUC-1 receptor positive
371 cancer cell lines including MCF-7 breast cancer cells[82]. AS1411 is a popular aptamer targeting the
372 nucleolin receptor, which is displayed on rapidly proliferating cells including various cancer cells
373 [85, 86]. These cell targeting aptamers are widely employed to functionalise DNA nanostructures
374 such as an icosahedral DNA nanostructure[100] or ring-shaped DNA nanostructure[101], both with
375 12-valent S2.2 decoration to deliver doxorubicin (Dox, dsDNA intercalating anti-cancer drug); A long
376 linear DNA nanostructure with a Sgc8c or an AS1411 motif to deliver Dox[102]; a fluorophore labelled
377 dendric DNA nanostructure with Sgc8c to specifically deliver Dox to cancer cells in vitro[103]; Y or
378 X shaped DNA nanostructures with Sgc8c, TC01 (aptamer targeting) and Sgc4f[104]; a tetrahedral
379 DNA nanostructure with trivalent AS1411 which reduces growth of cancer cells[105]; and another
380 DNA tetrahedron with both AS1411 and MUC-1 aptamers delivering Dox[106] along with many
381 others[107, 108].

382 It is noteworthy that nanoparticles in a certain size range are passively accumulated to solid
 383 cancer tumours by the enhanced permeability and retention (EPR) effect and then are taken in to cells
 384 by endocytosis[109], this is encouraging for DNA nanoscience as DNA origami structures are
 385 typically within this size range. So far a 30 helix bundle (HB) DNA origami tube decorated with 62-
 386 valent CpG motif for TLR9 mediated immune response[26]; 6HB tubular or triangular DNA origami
 387 structures carrying Dox[110], a twisted DNA origami tube with tuneable Dox capacity and releasing
 388 rate[111] and a 26HB rod-like DNA origami structure carrying daunorubicin[112] have been used to
 389 take advantage of this effect. A systematic comparison of cellular uptake efficiency among DNA
 390 nanostructures and 3D DNA origami structures with gold nanoparticles (AuNP)[113] have shown in
 391 vitro cell uptake of DNA origami structures, while in vivo passive accumulation and cellular intake
 392 of various shapes of naked DNA origami structures carrying Dox[114] or gold nanorod (AuNR)[115]
 393 as well as lipid membranes and PEG coated octahedral DNA origami structures[116] have been
 394 demonstrated.

395 Passive DNA origami delivery with Dox[110] or AuNRs[115], integrated with MUC-1 aptamer
 396 (S2.2) to enhance cell targeting of a triangular DNA origami structure has been reported, where the
 397 structure carries both Dox and AuNR as anticancer drugs (Figure 4A)[80]. AuNR synergistically
 398 suppressed the expression of P-glycoprotein and the growth of multidrug resistant MCF-7 cells upon
 399 NIR irradiation via the hyperthermia effect[117] and the work successfully demonstrated an aptamer
 400 derived cell intake enhancement of the DNA origami structure. Further development allowed
 401 attachment of two capped p53 gene modules to the triangular DNA origami carrying Dox, designed
 402 to be released and expressed after delivery into the cells, which was tested and showed efficacy in
 403 mice[118]. Another report utilised the C2NP aptamer, which recognises CD30 positive cancer cells
 404 including K299 and triggers a signalling pathway leading to apoptosis at high concentration[88]. S
 405 DNA rectangle decorated with four or sixteen such aptamers enhanced cell specific Dox delivery and
 406 apoptosis induction[87].
 407

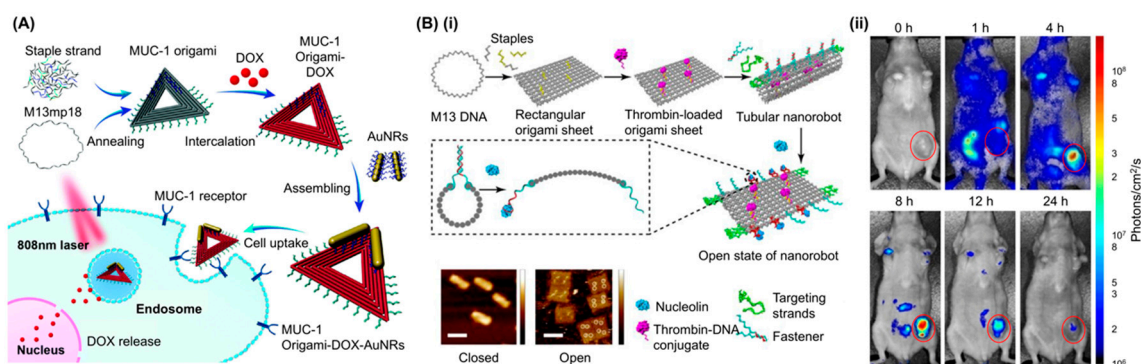


Figure 4. Examples of aptamer use in cell targeting of DNA origami. (A) Schematic showing that triangle DNA origami functionalized with the MUC-1 aptamer can load doxorubicin and carry AuNRs to inhibit the growth of resistant breast cancer cells. Triangular shaped DNA origami structure is hybridized with staple strands (grey), MUC-1 aptamer strands (green) and capture strands (blue). The multifunctional DNA nanostructures (MUC-1 aptamer–DNA origami–DOX–AuNRs complex, MODA) were administered to the MCF-7/ADR cells, and the photothermal effects were investigated. Adapted with permission from Song et al, *Nanoscale*, 2017[80]. (B) (i) (top) Schematic showing of the construction of thrombin-loaded nanorobot by DNA origami, and its reconfiguration into a rectangular DNA sheet in response to nucleolin binding. (bottom) AFM images of the DNA nanorobots in closed (left) and opened states (right). The four bright spots displayed on the surface of the origami sheet represent the thrombin molecules. (ii) In vivo experiment to show the activity of aptamer-based DNA nanorobots. Optical imaging of an MDA-MB-231 mouse bearing a human breast tumor before and after intravenous injection of Cy5.5-labeled nanorobot. A high-intensity fluorescent signal was detected only in the tumor region of

mice 8 h after injection. 0 h indicates before injection. Adapted with permission from Li et al, *Nat. Biotechnol.*, 2018[84].

408 Recently, an intelligent DNA origami nanorobot, that can target tumours in mice, inhibiting their
409 growth, has been reported (Figure 4B)[84]. In the design, the authors employed AS1411 not only for
410 targeting cancer cells, but also to regulate the mechanical transformation of the DNA nanorobot to
411 expose the cargo at the focus. They first loaded bioactive thrombin-DNA conjugates to four positions
412 of the same surface of a rectangular DNA origami structure by hybridisation. Then the DNA structure
413 was rolled and “fastened” by six pairs of AS1411 aptamer locks to form a hollow tube. The locks are
414 opened upon interaction with nucleolin. The nanorobot was further decorated with eight AS1411
415 strands to enhance cell targeting. Thrombin was kept inside the hollow structure to protect it from
416 the innate coagulation system during delivery and was exposed to surrounding only when the
417 nanorobot reached nucleolin positive cells, causing a coagulation cascade that eventually induces
418 necrosis of tumour tissue. Using MDA-MB-231 model mice bearing a human breast cancer tumour
419 as well as C57BL/6J mice injected with B16-F10 melanoma tumour cells, they successfully
420 demonstrated cancer tissue targeting, designed necrosis, tumour growth inhibition and enhancement
421 of survival time.

422 Conclusion and Perspective

423 In this review we have summarised the various examples wherein DNA aptamers have been
424 combined with DNA origami and noted that the work can be separated into four distinct areas. In
425 the first, aptamers are used as protein immobilisation modules capable of capturing and arranging
426 proteins in defined patterns and with defined order. This may even allow control and manipulation
427 of protein to produce designed protein-based nanomachines but on a DNA origami framework. The
428 second and the third areas show how aptamers can be used to initiate and control structural changes
429 in DNA origami, allowing extremely sensitive detection and linking the output of molecular logic
430 gates to conformational dynamism. Finally, cell targeting aptamers enable specificity of drug delivery
431 by DNA origami carriers. As listed in Table 1, the majority of the research relies on a limited number
432 of established aptamers to demonstrate feasibility of designs while some have utilised DNA origami
433 to expand the applications of newly developed aptamers[50, 70, 76, 78]. There are more aptamers,
434 both well-characterised or novel that are potentially useful for functionalisation of DNA origami
435 structures with various potential applications. Some have already been used in DNA nanostructure
436 research or other bioconjugate research reviewed elsewhere[4, 12, 38, 105]. As demonstrated by the
437 work replacing an ATP aptamer lock with a new split aptamer system to enhance efficiency of DNA
438 origami device transformation[71, 76], seeking alternative aptamers could overcome a general
439 problem, which is that the aptamer affinity generally decreases upon attachment to DNA origami.
440 This is likely due to steric and electrostatic effects. An intelligent DNA nanorobot with AS1411 for
441 both cell targeting and drug release[84] exemplifies the new possibility of development of
442 sophisticated DNA origami devices utilising multiple aptamers simultaneously to achieve synergistic
443 effects or programmability and we hope that this brief review encourages the further development
444 of improved aptamers for integration with DNA origami.
445

446 **Author Contributions:** JGH conceived and supervised writing of the paper. JGH, YS, MSI, MA, SCCS and JAT
447 all contributed to writing the paper.

448 **Funding:** JGH and MSI were funded by the Team Programme of the Foundation for Polish Science co-financed
449 by the European Union under the European Regional Development Fund (TEAM/2016-3/23) awarded to JGH.
450 YS and MA were supported by POLONEZ3 (2016/23/P/NZ1/04097) of Polish National Science Centre (NCN) co-
451 funded by the Marie Skłodowska-Curie action of the European Union (665778). SCCS and JAT have been funded
452 by grants from the General Research Fund (17119814) of the Hong Kong University Grants Council.

453 **Conflicts of Interest:** The authors declare no conflict of interest. The funders had no role in the design of the
454 study; in the collection, analyses, or interpretation of data; in the writing of the manuscript, or in the decision to
455 publish the results.

456 **References**

- 457 1. Ellington, A. D.; Szostak, J. W., In vitro selection of RNA molecules that bind specific ligands. *Nature*
458 **1990**, 346, (6287), 818-822.
- 459 2. Tuerk, C.; Gold, L., Systematic evolution of ligands by exponential enrichment: RNA ligands to
460 bacteriophage T4 DNA polymerase. *Science* **1990**, 249, (4968), 505-510.
- 461 3. Bock, L. C.; Griffin, L. C.; Latham, J. A.; Vermaas, E. H.; Toole, J. J., Selection of single-stranded DNA
462 molecules that bind and inhibit human thrombin. *Nature* **1992**, 355, (6360), 564-566.
- 463 4. Zhu, Q.; Liu, G.; Kai, M., DNA Aptamers in the Diagnosis and Treatment of Human Diseases. *Molecules*
464 **2015**, 20, (12), 20979-20997.
- 465 5. Morita, Y.; Leslie, M.; Kameyama, H.; Volk, D.; Tanaka, T., Aptamer Therapeutics in Cancer: Current
466 and Future. *Cancers* **2018**, 10, (3), 80-22.
- 467 6. Pieken, W. A.; Olsen, D. B.; Benseler, F.; Aurup, H.; Eckstein, F., Kinetic characterization of ribonuclease-
468 resistant 2'-modified hammerhead ribozymes. *Science* **1991**, 253, (5017), 314-317.
- 469 7. Cummins, L. L.; Owens, S. R.; Risen, L. M.; Lesnik, E. A.; Freier, S. M.; McGee, D.; Guinosso, C. J.; Cook,
470 P. D., Characterization of fully 2'-modified oligoribonucleotide hetero- and homoduplex hybridization
471 and nuclease sensitivity. *Nucleic Acids Res.* **1995**, 23, (11), 2019-2024.
- 472 8. Rohloff, J. C.; Gelinis, A. D.; Jarvis, T. C.; Ochsner, U. A.; Schneider, D. J.; Gold, L.; Janjic, N., Nucleic
473 Acid Ligands With Protein-like Side Chains: Modified Aptamers and Their Use as Diagnostic and
474 Therapeutic Agents. *Mol. Ther.* **2014**, 3, (Supplement C), e201.
- 475 9. Jarvis, T. C.; Davies, D. R.; Hisaminato, A.; Resnicow, D. I.; Gupta, S.; Waugh, S. M.; Nagabukuro, A.;
476 Wadatsu, T.; Hishigaki, H.; Gawande, B.; Zhang, C.; Wolk, S. K.; Mayfield, W. S.; Nakaishi, Y.; Burgin,
477 A. B.; Stewart, L. J.; Edwards, T. E.; Gelinis, A. D.; Schneider, D. J.; Janjic, N., Non-helical DNA Triplex
478 Forms a Unique Aptamer Scaffold for High Affinity Recognition of Nerve Growth Factor. *Struct.* **2015**,
479 23, (7), 1293-1304.
- 480 10. Ng, E. W. M.; Shima, D. T.; Calias, P.; Cunningham, E. T.; Guyer, D. R.; Adamis, A. P., Pegaptanib, a
481 targeted anti-VEGF aptamer for ocular vascular disease. *Nat. Rev. Drug Discov.* **2006**, 5, (2), 123-132.
- 482 11. Kourlas, H.; Schiller, D. S., Pegaptanib sodium for the treatment of neovascular age-related macular
483 degeneration: a review. *Clin. Ther.* **2006**, 28, (1), 36-44.
- 484 12. Lao, Y.-H.; Phua, K. K. L.; Leong, K. W., Aptamer Nanomedicine for Cancer Therapeutics: Barriers and
485 Potential for Translation. *ACS Nano* **2015**, 9, (3), 2235-2254.
- 486 13. Sundaram, P.; Kurniawan, H.; Byrne, M. E.; Wower, J., Therapeutic RNA aptamers in clinical trials. *Eur.*
487 *J. Pharm. Sci.* **2013**, 48, (1-2), 259-271.
- 488 14. Rothmund, P. W. K., Folding DNA to create nanoscale shapes and patterns. *Nature* **2006**, 440, (7082),
489 297-302.
- 490 15. Wang, P.; Meyer, T. A.; Pan, V.; Dutta, P. K.; Ke, Y., The Beauty and Utility of DNA Origami. *Chem.*
491 **2017**, 2, (3), 359-382.
- 492 16. Andersen, E. S.; Dong, M.; Nielsen, M. M.; Jahn, K.; Lind-Thomsen, A.; Mamdouh, W.; Gothelf, K. V.;
493 Besenbacher, F.; Kjems, J., DNA Origami Design of Dolphin-Shaped Structures with Flexible Tails. *ACS*
494 *Nano* **2008**, 2, (6), 1213-1218.
- 495 17. Chhabra, R.; Sharma, J.; Ke, Y.; Liu, Y.; Rinker, S.; Lindsay, S.; Yan, H., Spatially Addressable
496 Multiprotein Nanoarrays Templated by Aptamer-Tagged DNA Nanoarchitectures. *J. Am. Chem. Soc.*
497 **2007**, 129, (34), 10304-10305.
- 498 18. Ke, Y.; Lindsay, S.; Chang, Y.; Liu, Y.; Yan, H., Self-assembled water-soluble nucleic acid probe tiles for
499 label-free RNA hybridization assays. *Science* **2008**, 319, (5860), 180-183.
- 500 19. Williams, B. A. R.; Lund, K.; Liu, Y.; Yan, H.; Chaput, J. C., Self-Assembled Peptide Nanoarrays: An
501 Approach to Studying Protein-Protein Interactions. *Angew. Chem. Int. Ed.* **2007**, 46, (17), 3051-3054.
- 502 20. Sharma, J.; Chhabra, R.; Andersen, C. S.; Gothelf, K. V.; Yan, H.; Liu, Y., Toward reliable gold
503 nanoparticle patterning on self-assembled DNA nanoscaffold. *J. Am. Chem. Soc.* **2008**, 130, (25), 7820-1.
- 504 21. Schnitzbauer, J.; Strauss, M. T.; Schlichthaerle, T.; Schueder, F.; Jungmann, R., Super-resolution
505 microscopy with DNA-PAINT. *Nat. Protoc.* **2017**, 12, (6), 1198-1228.
- 506 22. Steinhauer, C.; Jungmann, R.; Sobey, T. L.; Simmel, F. C.; Tinnefeld, P., DNA Origami as a Nanoscopic
507 Ruler for Super-Resolution Microscopy. *Angew. Chem. Int. Ed.* **2009**, 48, (47), 8870-8873.
- 508 23. Yamazaki, T.; Heddle, J. G.; Kuzuya, A.; Komiyama, M., Orthogonal enzyme arrays on a DNA origami
509 scaffold bearing size-tunable wells. *Nanoscale* **2014**, 6, (15), 9122-5.

- 510 24. Hong, F.; Zhang, F.; Liu, Y.; Yan, H., DNA Origami: Scaffolds for Creating Higher Order Structures.
511 *Chem. Rev.* **2017**, *117*, (20), 12584-12640.
- 512 25. Andersen, E. S.; Dong, M.; Nielsen, M. M.; Jahn, K.; Subramani, R.; Mamdouh, W.; Golas, M. M.; Sander,
513 B.; Stark, H.; Cristiano, L. P. O.; Pedersen, J. S.; Birkedal, V.; Besenbacher, F.; Gothelf, K. V.; Kjems, J.,
514 Self-assembly of a nanoscale DNA box with a controllable lid. *Nature* **2009**, *459*, (7243), 73-76.
- 515 26. Schüller, V. J.; Heidegger, S.; Sandholzer, N.; Nickels, P. C.; Suhartha, N. A.; Endres, S.; Bourquin, C.;
516 Liedl, T., Cellular Immunostimulation by CpG-Sequence-Coated DNA Origami Structures. *ACS Nano*
517 **2011**, *5*, (12), 9696-9702.
- 518 27. Kuzyk, A.; Schreiber, R.; Fan, Z.; Pardatscher, G.; Roller, E.-M.; Högele, A.; Simmel, F. C.; Govorov, A.
519 O.; Liedl, T., DNA-based self-assembly of chiral plasmonic nanostructures with tailored optical
520 response. *Nature* **2012**, *483*, (7389), 311-314.
- 521 28. Tan, L. H.; Xing, H.; Lu, Y., DNA as a powerful tool for morphology control, spatial positioning, and
522 dynamic assembly of nanoparticles. *Acc. Chem. Res.* **2014**, *47*, (6), 1881-1890.
- 523 29. Liu, J.; Lee, J. H.; Lu, Y., Quantum Dot Encoding of Aptamer-Linked Nanostructures for One-Pot
524 Simultaneous Detection of Multiple Analytes. *Anal. Chem.* **2007**, *79*, (11), 4120-4125.
- 525 30. Liu, J.; Lu, Y., Smart Nanomaterials Responsive to Multiple Chemical Stimuli with Controllable
526 Cooperativity. *Adv. Mater.* **2006**, *18*, (13), 1667-1671.
- 527 31. Mo, R.; Jiang, T.; DiSanto, R.; Tai, W.; Gu, Z., ATP-triggered anticancer drug delivery. *Nat. Commun.*
528 **2014**, *5*, 1-10.
- 529 32. Liao, W.-C.; Lu, C.-H.; Hartmann, R.; Wang, F.; Sohn, Y. S.; Parak, W. J.; Willner, I., Adenosine
530 Triphosphate-Triggered Release of Macromolecular and Nanoparticle Loads from Aptamer/DNA-
531 Cross-Linked Microcapsules. *ACS Nano* **2015**, *9*, (9), 9078-9086.
- 532 33. Yang, F.; Li, Q.; Wang, L.; Zhang, G.-J.; Fan, C., Framework-Nucleic-Acid-Enabled Biosensor
533 Development. *ACS Sens.* **2018**, *3*, (5), 903-919.
- 534 34. Li, J.; Green, A. A.; Yan, H.; Fan, C., Engineering nucleic acid structures for programmable molecular
535 circuitry and intracellular biocomputation. *Nat. Rev. Clin. Oncol.* **2017**, 1-12.
- 536 35. Seeman, N. C.; Sleiman, H. F., DNA nanotechnology. *Nat. Rev. Clin. Oncol.* **2017**, *3*, (1), 1-23.
- 537 36. Hu, Q.; Li, H.; Wang, L.; Gu, H.; Fan, C., DNA Nanotechnology-Enabled Drug Delivery Systems. *Chem.*
538 *Rev.* **2018**, acs.chemrev.7b00663-48.
- 539 37. Chen, A.; Yan, M.; Yang, S., Split aptamers and their applications in sandwich aptasensors. *Trends Anal.*
540 *Chem.* **2016**, *80*, (C), 581-593.
- 541 38. Meng, H.-M.; Liu, H.; Kuai, H.; Peng, R.; Mo, L.; Zhang, X.-B., Aptamer-integrated DNA nanostructures
542 for biosensing, bioimaging and cancer therapy. *Chem. Soc. Rev.* **2016**, *45*, 2583-2602.
- 543 39. Shiu, S. C.-C.; Kinghorn, A. B.; Sakai, Y.; Cheung, Y.-W.; Heddle, J. G.; Tanner, J. A., The Three S's for
544 Aptamer-Mediated Control of DNA Nanostructure Dynamics: Shape, Self-Complementarity, and
545 Spatial Flexibility. *Chem. BioChem.* **2018**, *19*, (18), 1900-1906.
- 546 40. Alivisatos, A. P.; Johnsson, K. P.; Peng, X.; Wilson, T. E.; Loweth, C. J.; Bruchez, M. P.; Schultz, P. G.,
547 Organization of 'nanocrystal molecules' using DNA. *Nature* **1996**, *382*, (6592), 609-611.
- 548 41. Yan, H.; Park, S. H.; Finkelstein, G.; Reif, J. H.; LaBean, T. H., DNA-templated self-assembly of protein
549 arrays and highly conductive nanowires. *Science* **2003**, *301*, (5641), 1882-1884.
- 550 42. Niemeyer, C. M.; Bürger, W.; Peplies, J., Covalent DNA-Streptavidin Conjugates as Building Blocks for
551 Novel Biometallic Nanostructures. *Angew. Chem. Int. Ed.* **1998**, *37*, (16), 2265-2268.
- 552 43. Liu, Y.; Lin, C.; Li, H.; Yan, H., Aptamer-Directed Self-Assembly of Protein Arrays on a DNA
553 Nanostructure. *Angew. Chem. Int. Ed.* **2005**, *44*, (28), 4333-4338.
- 554 44. Green, L. S.; Jellinek, D.; Jenison, R.; Ostman, A.; Heldin, C. H.; Janjic, N., Inhibitory DNA ligands to
555 platelet-derived growth factor B-chain. *Biochemistry* **1996**, *35*, (45), 14413-14424.
- 556 45. Tasset, D. M.; Kubik, M. F.; Steiner, W., Oligonucleotide inhibitors of human thrombin that bind distinct
557 epitopes. *J. Mol. Biol.* **1997**, *272*, (5), 688-698.
- 558 46. Rinker, S.; Ke, Y.; Liu, Y.; Chhabra, R.; Yan, H., Self-assembled DNA nanostructures for distance-
559 dependent multivalent ligand-protein binding. *Nat. Nanotechnol.* **2008**, *3*, (7), 418-422.
- 560 47. Mei, Q.; Johnson, R. H.; Wei, X.; Su, F.; Liu, Y.; Kelbauskas, L.; Lindsay, S.; Meldrum, D. R.; Yan, H., On-
561 chip isotachopheresis separation of functional DNA origami capture nanoarrays from cell lysate. *Nano*
562 *Res.* **2013**, *6*, (10), 712-719.

- 563 48. Diener, J. L.; Wagner-Whyte, J.; Fontana, D.; Corp, A., Aptamers that bind thrombin with high affinity.
564 *United States Patent* **2011**, US 7,998,939 B2
- 565 49. Kumar, N.; Seminario, J. M., Molecular dynamics study of thrombin capture by aptamers TBA26 and
566 TBA29 coupled to a DNA origami. *Mol. Simulat.* **2018**, *44*, (9), 749-756.
- 567 50. Godonoga, M.; Lin, T.-Y.; Oshima, A.; Sumitomo, K.; Tang, M. S. L.; Cheung, Y.-W.; Kinghorn, A. B.;
568 Dirkzwager, R. M.; Zhou, C.; Kuzuya, A.; Tanner, J. A.; Heddle, J. G., A DNA aptamer recognising a
569 malaria protein biomarker can function as part of a DNA origami assembly. *Sci. Rep.* **2016**, *6*, (1), 21266.
- 570 51. Lu, Z.; Wang, Y.; Xu, D.; Pang, L., Aptamer-tagged DNA origami for spatially addressable detection of
571 aflatoxin B1. *Chem. Commun. (Camb.)* **2017**, *53*, (5), 941-944.
- 572 52. Tintoré, M.; Gállego, I.; Manning, B.; Eritja, R.; Fàbrega, C., DNA Origami as a DNA Repair Nanosensor
573 at the Single-Molecule Level. *Angew. Chem. Int. Ed.* **2013**, *52*, (30), 7747-7750.
- 574 53. Cheung, Y.-W.; Kwok, J.; Law, A. W. L.; Watt, R. M.; Kotaka, M.; Tanner, J. A., Structural basis for
575 discriminatory recognition of Plasmodium lactate dehydrogenase by a DNA aptamer. *Proc. Natl. Acad.*
576 *Sci.* **2013**, *110*, (40), 15967-15972.
- 577 54. Li, F.; Chen, H.; Pan, J.; Cha, T.-G.; Medintz, I. L.; Choi, J. H., A DNzyme-mediated logic gate for
578 programming molecular capture and release on DNA origami. *Chem. Commun.* **2016**, *52*, (54), 8369-8372.
- 579 55. Le, L. C.; Cruz-Aguado, J. A.; Penner, G. A.; Limited, N. B., DNA ligands for aflatoxin and zearalenone.
580 *United States Patents* **2011**, US 2012/0225494 A1. .
- 581 56. Daems, D.; Pfeifer, W.; Rutten, I.; Saccà, B.; Spasic, D.; Lammertyn, J., Three-Dimensional DNA Origami
582 as Programmable Anchoring Points for Bioreceptors in Fiber Optic Surface Plasmon Resonance
583 Biosensing. *ACS Appl. Mater. Interfaces* **2018**, *10*, (28), 23539-23547.
- 584 57. Rajendran, A.; Nakata, E.; Nakano, S.; Morii, T., Nucleic-Acid-Templated Enzyme Cascades. *Chem. Eur.*
585 *J. of Chem. Bio.* **2017**, *18*, (8), 696-716.
- 586 58. Fu, J.; Liu, M.; Liu, Y.; Woodbury, N. W.; Yan, H., Interenzyme Substrate Diffusion for an Enzyme
587 Cascade Organized on Spatially Addressable DNA Nanostructures. *J. Am. Chem. Soc.* **2012**, *134*, (12),
588 5516-5519.
- 589 59. Nakata, E.; Liew, F. F.; Uwatoko, C.; Kiyonaka, S.; Mori, Y.; Katsuda, Y.; Endo, M.; Sugiyama, H.; Morii,
590 T., Zinc-Finger Proteins for Site-Specific Protein Positioning on DNA-Origami Structures. *Angew. Chem.*
591 *Int. Ed.* **2012**, *51*, (10), 2421-2424.
- 592 60. Ngo, T. A.; Nakata, E.; Saimura, M.; Kodaki, T.; Morii, T., A protein adaptor to locate a functional
593 protein dimer on molecular switchboard. *Methods* **2014**, *67*, (2), 142-150.
- 594 61. Ngo, T. A.; Nakata, E.; Saimura, M.; Morii, T., Spatially Organized Enzymes Drive Cofactor-Coupled
595 Cascade Reactions. *J. Am. Chem. Soc.* **2016**, *138*, (9), 3012-3021.
- 596 62. Kurokawa, T.; Kiyonaka, S.; Nakata, E.; Endo, M.; Koyama, S.; Mori, E.; Tran, N. H.; Dinh, H.; Suzuki,
597 Y.; Hidaka, K.; Kawata, M.; Sato, C.; Sugiyama, H.; Morii, T.; Mori, Y., DNA Origami Scaffolds as
598 Templates for Functional Tetrameric Kir3 K⁺ Channels. *Angew. Chem. Int. Ed.* **2018**, *57*, (10), 2586-2591.
- 599 63. Douglas, S. M.; Bachelet, I.; Church, G. M., A logic-gated nanorobot for targeted transport of molecular
600 payloads. *Science* **2012**, *335*, (6070), 831-834.
- 601 64. Koirala, D.; Shrestha, P.; Emura, T.; Hidaka, K.; Mandal, S.; Endo, M.; Sugiyama, H.; Mao, H., Single-
602 Molecule Mechanochemical Sensing Using DNA Origami Nanostructures. *Angew. Chem. Int. Ed.* **2014**,
603 *53*, (31), 8137-8141.
- 604 65. Amir, Y.; Ben-Ishay, E.; Levner, D.; Ittah, S.; Abu-Horowitz, A.; Bachelet, I., Universal computing by
605 DNA origami robots in a living animal. *Nat. Nanotechnol.* **2014**, *9*, (5), 353-357.
- 606 66. Kaur, H.; Yung, L.-Y. L., Probing High Affinity Sequences of DNA Aptamer against VEGF165. *PLoS*
607 *ONE* **2012**, *7*, (2), e31196-9.
- 608 67. Tang, Z.; Shangguan, D.; Wang, K.; Shi, H.; Sefah, K.; Mallikratchy, P.; Chen, H. W.; Li, Y.; Tan, W.,
609 Selection of Aptamers for Molecular Recognition and Characterization of Cancer Cells. *Anal. Chem.*
610 **2007**, *79*, (13), 4900-4907.
- 611 68. Shangguan, D.; Tang, Z.; Mallikratchy, P.; Xiao, Z.; Tan, W., Optimization and Modifications of
612 Aptamers Selected from Live Cancer Cell Lines. *Chem. Eur. J. of Chem. Bio.* **2007**, *8*, (6), 603-606.
- 613 69. Shangguan, D.; Cao, Z.; Meng, L.; Mallikratchy, P.; Sefah, K.; Wang, H.; Li, Y.; Tan, W., Cell-Specific
614 Aptamer Probes for Membrane Protein Elucidation in Cancer Cells. *J. Proteome Res.* **2008**, *7*, (5), 2133-
615 2139.

- 616 70. Tang, M. S. L.; Shiu, S. C.-C.; Godonoga, M.; Cheung, Y.-W.; Liang, S.; Dirkwager, R. M.; Kinghorn, A.
617 B.; Fraser, L. A.; Heddle, J. G.; Tanner, J. A., An aptamer-enabled DNA nanobox for protein sensing.
618 *Nanomed. Nanotechnol.* **2018**, *14*, (4), 1161-1168.
- 619 71. Kuzuya, A.; Sakai, Y.; Yamazaki, T.; Xu, Y.; Komiyama, M., Nanomechanical DNA origami 'single-
620 molecule beacons' directly imaged by atomic force microscopy. *Nat. Commun.* **2011**, *2*, (1), 449.
- 621 72. Yang, J.; Jiang, S.; Liu, X.; Pan, L.; Zhang, C., Aptamer-Binding Directed DNA Origami Pattern for Logic
622 Gates. *ACS Appl. Mater. Interfaces* **2016**, *8*, (49), 34054-34060.
- 623 73. Wu, N.; Willner, I., Programmed dissociation of dimer and trimer origami structures by aptamer-ligand
624 complexes. *Nanoscale* **2017**, *9*, (4), 1416-1422.
- 625 74. Huizenga, D. E.; Szostak, J. W., A DNA aptamer that binds adenosine and ATP. *Biochemistry* **1995**, *34*,
626 (2), 656-665.
- 627 75. Lin, C. H.; Patel, D. J., Structural basis of DNA folding and recognition in an AMP-DNA aptamer
628 complex: distinct architectures but common recognition motifs for DNA and RNA aptamers complexed
629 to AMP. *Chem. Biol.* **1997**, *4*, (11), 817-832.
- 630 76. Walter, H.-K.; Bauer, J.; Steinmeyer, J.; Kuzuya, A.; Niemeyer, C. M.; Wagenknecht, H.-A., "DNA
631 Origami Traffic Lights" with a Split Aptamer Sensor for a Bicolor Fluorescence Readout. *Nano Lett.* **2017**,
632 *17*, (4), 2467-2472.
- 633 77. Walter, H.-K.; Bohländer, P. R.; Wagenknecht, H.-A., Development of a Wavelength-Shifting
634 Fluorescent Module for the Adenosine Aptamer Using Photostable Cyanine Dyes. *ChemistryOpen* **2015**,
635 *4*, (2), 92-96.
- 636 78. Takeuchi, Y.; Endo, M.; Suzuki, Y.; Hidaka, K.; Durand, G.; Dausse, E.; Toulme, J. J.; Sugiyama, H.,
637 Single-molecule observations of RNA-RNA kissing interactions in a DNA nanostructure. *Biomater. Sci.*
638 **2016**, *4*, (1), 130-135.
- 639 79. Durand, G.; Lisi, S.; Ravelet, C.; Dausse, E.; Peyrin, E.; Toulmé, J.-J., Riboswitches Based on Kissing
640 Complexes for the Detection of Small Ligands. *Angew. Chem. Int. Ed.* **2014**, *53*, (27), 6942-6945.
- 641 80. Song, L.; Jiang, Q.; Liu, J.; Li, N.; Liu, Q.; Dai, L.; Gao, Y.; Liu, W.; Liu, D.; Ding, B., DNA origami/gold
642 nanorod hybrid nanostructures for the circumvention of drug resistance. *Nanoscale* **2017**, *9*, (23), 7750-
643 7754.
- 644 81. Chaithongyot, S.; Chomanee, N.; Charngkaew, K.; Udomprasert, A.; Kangsamaksin, T., Aptamer-
645 functionalized DNA nanosphere as a stimuli-responsive nanocarrier. *Mater. Lett.* **2018**, *214*, 72-75.
- 646 82. Ferreira, C. S. M.; Matthews, C. S.; Missailidis, S., DNA aptamers that bind to MUC1 tumour marker:
647 design and characterization of MUC1-binding single-stranded DNA aptamers. *Tumour Biol.* **2006**, *27*,
648 (6), 289-301.
- 649 83. Liu, J.; Lu, Y., Fast Colorimetric Sensing of Adenosine and Cocaine Based on a General Sensor Design
650 Involving Aptamers and Nanoparticles. *Angew. Chem. Int. Ed.* **2006**, *45*, (1), 90-94.
- 651 84. Li, S.; Jiang, Q.; Liu, S.; Zhang, Y.; Tian, Y.; Song, C.; Wang, J.; Zou, Y.; Anderson, G. J.; Han, J.-Y.; Chang,
652 Y.; Liu, Y.; Zhang, C.; Chen, L.; Zhou, G.; Nie, G.; Yan, H.; Ding, B.; Zhao, Y., A DNA nanorobot
653 functions as a cancer therapeutic in response to a molecular trigger in vivo. *Nat. Chem.* **2018**, *36*, (3), 258-
654 264.
- 655 85. Girvan, A. C.; Teng, Y.; Casson, L. K.; Thomas, S. D.; Jülicher, S.; Ball, M. W.; Klein, J. B.; Pierce, W. M.;
656 Barve, S. S.; Bates, P. J., AGRO100 inhibits activation of nuclear factor-kappaB (NF-kappaB) by forming
657 a complex with NF-kappaB essential modulator (NEMO) and nucleolin. *Mol. Cancer Ther.* **2006**, *5*, (7),
658 1790-1799.
- 659 86. Ireson, C. R.; Kelland, L. R., Discovery and development of anticancer aptamers. *Mol. Cancer Ther.* **2006**,
660 *5*, (12), 2957-2962.
- 661 87. Sun, P.; Zhang, N.; Tang, Y.; Yang, Y.; Zhou, J.; Zhao, Y., Site-specific anchoring aptamer C2NP on DNA
662 origami nanostructures for cancer treatment. *RSC Adv.* **2018**, *8*, (46), 26300-26308.
- 663 88. Parekh, P.; Kamble, S.; Zhao, N.; Zeng, Z.; Portier, B. P.; Zu, Y., Immunotherapy of CD30-expressing
664 lymphoma using a highly stable ssDNA aptamer. *Biomaterials* **2013**, *34*, (35), 8909-8917.
- 665 89. Hasegawa, H.; Sode, K.; Ikebukuro, K., Selection of DNA aptamers against VEGF165 using a protein
666 competitor and the aptamer blotting method. *Biotechnol. Lett.* **2008**, *30*, (5), 829-834.
- 667 90. Stojanovic, M. N.; de Prada, P.; Landry, D. W., Aptamer-Based Folding Fluorescent Sensor for Cocaine.
668 *J. Am. Chem. Soc.* **2001**, *123*, (21), 4928-4931.
- 669 91. Nutiu, R.; Li, Y., Structure-Switching Signaling Aptamers. *J. Am. Chem. Soc.* **2003**, *125*, (16), 4771-4778.

- 670 92. Stojanovic, M. N.; de Prada, P.; Landry, D. W., Fluorescent Sensors Based on Aptamer Self-Assembly.
671 *J. Am. Chem. Soc.* **2000**, *122*, (46), 11547-11548.
- 672 93. Koirala, D.; Yu, Z.; Dhakal, S.; Mao, H., Detection of Single Nucleotide Polymorphism Using Tension-
673 Dependent Stochastic Behavior of a Single-Molecule Template. *J. Am. Chem. Soc.* **2011**, *133*, (26), 9988-
674 9991.
- 675 94. Yurke, B.; Turberfield, A. J.; Mills, A. P.; Simmel, F. C.; Neumann, J. L., A DNA-fuelled molecular
676 machine made of DNA. *Nature* **2000**, *406*, (6796), 605-608.
- 677 95. Han, D.; Pal, S.; Nangreave, J.; Deng, Z.; Liu, Y.; Yan, H., DNA origami with complex curvatures in
678 three-dimensional space. *Science* **2011**, *332*, (6027), 342-346.
- 679 96. Liu, Z.; Tian, C.; Yu, J.; Li, Y.; Jiang, W.; Mao, C., Self-Assembly of Responsive Multilayered DNA
680 Nanocages. *J. Am. Chem. Soc.* **2015**, *137*, (5), 1730-1733.
- 681 97. Yang, Y.; Endo, M.; Hidaka, K.; Sugiyama, H., Photo-Controllable DNA Origami Nanostructures
682 Assembling into Predesigned Multiorientational Patterns. *J. Am. Chem. Soc.* **2012**, *134*, (51), 20645-20653.
- 683 98. Sefah, K.; Shangguan, D.; Xiong, X.; O'Donoghue, M. B.; Tan, W., Development of DNA aptamers using
684 Cell-SELEX. *Nat. Protoc.* **2010**, *5*, (6), 1169-1185.
- 685 99. Kim, M.; Kim, D.-M.; Kim, K.-S.; Jung, W.; Kim, D.-E., Applications of Cancer Cell-Specific Aptamers
686 in Targeted Delivery of Anticancer Therapeutic Agents. *Molecules* **2018**, *23*, (4), 830-20.
- 687 100. Chang, M.; Yang, C.-S.; Huang, D.-M., Aptamer-conjugated DNA icosahedral nanoparticles as a carrier
688 of doxorubicin for cancer therapy. *ACS Nano* **2011**, *5*, (8), 6156-6163.
- 689 101. Srivithya, V.; Roun, H.; Babu, M. S.; Hyung, P. J.; Ha, P. S., Aptamer-conjugated DNA nano-ring as the
690 carrier of drug molecules. *Nanotechnology* **2018**, *29*, (9), 095602.
- 691 102. Zhu, G.; Zheng, J.; Song, E.; Donovan, M.; Zhang, K.; Liu, C.; Tan, W., Self-assembled, aptamer-tethered
692 DNA nanotrains for targeted transport of molecular drugs in cancer theranostics. *Proc. Natl. Acad. Sci.*
693 **2013**, *110*, (20), 7998-8003.
- 694 103. Zhang, H.; Ma, Y.; Xie, Y.; An, Y.; Huang, Y.; Zhu, Z.; Yang, C. J., A Controllable Aptamer-Based Self-
695 Assembled DNA Dendrimer for High Affinity Targeting, Bioimaging and Drug Delivery. *Sci. Rep.* **2015**,
696 1-8.
- 697 104. You, M.; Peng, L.; Shao, N.; Zhang, L.; Qiu, L.; Cui, C.; Tan, W., DNA "Nano-Claw": Logic-Based
698 Autonomous Cancer Targeting and Therapy. *J. Am. Chem. Soc.* **2014**, *136*, (4), 1256-1259.
- 699 105. Charoenphol, P.; Bermudez, H., Aptamer-targeted DNA nanostructures for therapeutic delivery. *Mol.*
700 *Pharm.* **2014**, *11*, (5), 1721-1725.
- 701 106. Liu, X.; Wu, L.; Wang, L.; Jiang, W., A dual-targeting DNA tetrahedron nanocarrier for breast cancer
702 cell imaging and drug delivery. *Talanta* **2018**, *179*, 356-363.
- 703 107. Liu, J.; Wei, T.; Zhao, J.; Huang, Y.; Deng, H.; Kumar, A.; Wang, C.; Liang, Z.; Ma, X.; Liang, X.-J.,
704 Multifunctional aptamer-based nanoparticles for targeted drug delivery to circumvent cancer
705 resistance. *Biomaterials* **2016**, *91*, (C), 44-56.
- 706 108. Li, Q. S.; Zhao, D.; Shao, X. R.; Lin, S. Y.; Xie, X. P.; Liu, M. T.; Ma, W. J.; Shi, S. R.; Lin, Y. F., Aptamer-
707 Modified Tetrahedral DNA Nanostructure for Tumor-Targeted Drug Delivery. *ACS Appl. Mater.*
708 *Interfaces* **2017**, *9*, (42), 36695-36701.
- 709 109. Jain, R. K.; Stylianopoulos, T., Delivering nanomedicine to solid tumors. *Nat. Rev. Clin. Oncol.* **2010**, *7*,
710 (11), 653-664.
- 711 110. Jiang, Q.; Song, C.; Nangreave, J.; Liu, X.; Lin, L.; Qiu, D.; Wang, Z.-G.; Zou, G.; Liang, X.; Yan, H.; Ding,
712 B., DNA origami as a carrier for circumvention of drug resistance. *J. Am. Chem. Soc.* **2012**, *134*, (32),
713 13396-13403.
- 714 111. Zhao, Y.-X.; Shaw, A.; Zeng, X.; Benson, E.; Nyström, A. M.; Högberg, B., DNA origami delivery system
715 for cancer therapy with tunable release properties. *ACS Nano* **2012**, *6*, (10), 8684-8691.
- 716 112. Halley, P. D.; Lucas, C. R.; McWilliams, E. M.; Webber, M. J.; Patton, R. A.; Kural, C.; Lucas, D. M.; Byrd,
717 J. C.; Castro, C. E., Daunorubicin-Loaded DNA Origami Nanostructures Circumvent Drug-Resistance
718 Mechanisms in a Leukemia Model. *Small* **2015**, *12*, (3), 308-320.
- 719 113. Wang, P.; Rahman, M. A.; Zhao, Z.; Weiss, K.; Zhang, C.; Chen, Z.; Hurwitz, S. J.; Chen, Z. G.; Shin, D.
720 M.; Ke, Y., Visualization of the Cellular Uptake and Trafficking of DNA Origami Nanostructures in
721 Cancer Cells. *J. Am. Chem. Soc.* **2018**, *140*, (7), 2478-2484.
- 722 114. Zhang, Q.; Jiang, Q.; Li, N.; Dai, L.; Liu, Q.; Song, L.; Wang, J.; Li, Y.; Tian, J.; Ding, B.; Du, Y., DNA
723 origami as an in vivo drug delivery vehicle for cancer therapy. *ACS Nano* **2014**, *8*, (7), 6633-6643.

- 724 115. Jiang, Q.; Shi, Y.; Zhang, Q.; Li, N.; Zhan, P.; Song, L.; Dai, L.; Tian, J.; Du, Y.; Cheng, Z.; Ding, B., A Self-
725 Assembled DNA Origami-Gold Nanorod Complex for Cancer Theranostics. *Small* **2015**, *11*, (38), 5134-
726 5141.
- 727 116. Perrault, S. D.; Shih, W. M., Virus-Inspired Membrane Encapsulation of DNA Nanostructures To
728 Achieve In Vivo Stability. *ACS Nano* **2014**, *8*, (5), 5132-5140.
- 729 117. Huang, X.; Jain, P. K.; El-Sayed, I. H.; El-Sayed, M. A., Plasmonic photothermal therapy (PPTT) using
730 gold nanoparticles. *Lasers Med. Sci.* **2007**, *23*, (3), 217-228.
- 731 118. Liu, J.; Song, L.; Liu, S.; Jiang, Q.; Liu, Q.; Li, N.; Wang, Z.-G.; Ding, B., A DNA-Based Nanocarrier for
732 Efficient Gene Delivery and Combined Cancer Therapy. *Nano Lett.* **2018**, *18*, (6), 3328-3334.